HHS Public Access

Author manuscript

J Mol Cell Cardiol. Author manuscript; available in PMC 2022 August 01.

Published in final edited form as:

J Mol Cell Cardiol. 2021 August ; 157: 31–44. doi:10.1016/j.yjmcc.2021.04.005.

Branched Chain Amino Acids Selectively Promote Cardiac Growth at the End of the Awake Period

Mary N. Latimer[1], **Ravi Sonkar**[2], **Sobuj Mia**[1], **Isabelle Robillard Frayne**[3], **Karen J. Carter**[1], **Christopher A. Johnson**[1], **Samir Rana**[1], **Min Xie**[1], **Glenn C. Rowe**[1], **Adam R. Wende**[4], **Sumanth D. Prabhu**[1], **Stuart J. Frank**[2,5], **Christine Des Rosiers**[3], **John C. Chatham**[4], **Martin E. Young**[1]

[1]Division of Cardiovascular Disease, Department of Medicine, University of Alabama at Birmingham, Birmingham, Alabama, USA.

[2]Division of Endocrinology, Diabetes and Metabolism, Department of Medicine, University of Alabama at Birmingham, Birmingham, Alabama, USA.

[3]Department of Nutrition, Université de Montréal and Montreal Heart Institute, Montréal, Québec, Canada.

[4]Division of Molecular Cellular Pathology, Department of Pathology, University of Alabama at Birmingham, Birmingham, Alabama, USA.

[5]Endocrinology Section, Birmingham VAMC Medical Service, Birmingham, Alabama, USA.

Abstract

Essentially all biological processes fluctuate over the course of the day, manifesting as time-of-day-dependent variations with regards to the way in which organ systems respond to normal behaviors. For example, basic, translational, and epidemiologic studies indicate that temporal partitioning of metabolic processes governs the fate of dietary nutrients, in a manner in which concentrating caloric intake towards the end of the day is detrimental to both cardiometabolic and cardiovascular parameters. Despite appreciation that branched chain amino acids impact risk for obesity, diabetes mellitus, and heart failure, it is currently unknown whether the time-of-day at which dietary BCAAs are consumed influence cardiometabolic/cardiovascular outcomes. Here, we report that feeding mice a BCAA-enriched meal at the end of the active period (i.e., last 4hrs of the dark phase) rapidly increases cardiac protein synthesis and mass, as well as cardiomyocyte size; consumption of the same meal at the beginning of the active period (i.e., first 4hrs of the dark

Address for correspondence: Martin E. Young, D.Phil., Division of Cardiovascular Disease, Department of Medicine, University of Alabama at Birmingham, 703 19th St. S., ZRB 308, Birmingham, Alabama, 35294, USA, Tel # 205-934-2328, Fax # 205-975-5104, meyoung@uab.edu.

[6]AUTHOR CONTRIBUTIONS

M.N. Latimer, S.D. Prabhu, S. Frank, J.C. Chatham, C. Des Rosiers, and M.E. Young designed research; M.N. Latimer, R. Sonkar, S. Mia, I. F. Robillard, C.A. Johnson, S. Rana, M. Xie, G.C. Rowe, A.R. Wende, and M.E. Young performed research; M.N. Latimer, R. Sonkar, I.F. Robillard, and M.E. Young analyzed data; M.N. Latimer, C. Des Rosiers, J.C. Chatham, and M.E. Young wrote the manuscript.

phase) is without effect. This was associated with a greater BCAA-induced activation of mTOR signaling in the heart at the end of the active period; pharmacological inhibition of mTOR (through rapamycin) blocked BCAA-induced augmentation of cardiac mass and cardiomyocyte size. Moreover, genetic disruption of the cardiomyocyte circadian clock abolished time-of-day-dependent fluctuations in BCAA-responsiveness. Finally, we report that repetitive consumption of BCAA-enriched meals at the end of the active period accelerated adverse cardiac remodeling and contractile dysfunction in mice subjected to transverse aortic constriction. Thus, our data demonstrate that the timing of BCAA consumption has significant implications for cardiac health and disease.

Keywords

Chronobiology; Hypertrophy; Nutrition; Protein Synthesis; Signaling

1. INTRODUCTION

Significant environmental/behavioral changes have occurred over the last several decades, in association with increased cardiometabolic (e.g., obesity, diabetes) and cardiovascular diseases (19). These include introduction of energy dense and highly palatable foods, reduced physical activity, and decreased sleep duration. A complex interplay likely exists between many of these risk factors. Recent epidemiologic studies suggest that the time-of-day at which calorically-dense meals are consumed impacts cardiometabolic/cardiovascular disease incidence and progression, leading to recommendations that “eating a greater share of the total calorie intake earlier in the day to have positive effects on risk factors for heart disease and diabetes mellitus” (American Heart Association Scientific Statement) (35). Considerable progress has been made in this field, suggesting that the metabolic fate of dietary nutrients is dependent of time-of-day (3). However, many unanswered questions remain, including whether all nutrients should be considered equal with regards to optimal time-of-day of consumption.

Of the major metabolic alterations reported in cardiometabolic/cardiovascular disease states, perturbed branched chain amino acid (BCAA; leucine, isoleucine, and valine) catabolism has received appreciable attention recently. Observational studies in humans report elevated plasma BCAA levels during obesity and diabetes mellitus, as well as multiple cardiovascular disease states (25, 28, 37, 43). Modulating dietary BCAA levels in preclinical models impacts adiposity, glucose tolerance, and insulin sensitivity (13, 24). Moreover, genetic and pharmacologic manipulation of BCAA catabolism in mice invariably impacts cardiometabolic parameters and cardiac disease progression (24, 36). BCAA influence cellular/organ functions through multiple mechanisms, including activation of mTOR (mammalian target of rapamycin), a kinase governing critical biological functions (e.g., protein synthesis) that has been linked with cardiometabolic health and lifespan (10, 44). mTOR activity fluctuates across the day in multiple organs; in the heart, peak activity is observed at the awake-to-sleep transition, a time at which protein synthesis is augmented (26). Emerging evidence suggests that daily rhythms in mTOR activity are mediated by circadian clocks; cardiomyocyte-specific deletion of the core clock component BMAL1

(brain and muscle ARNT-like protein 1; encoded by *Arntl*) not only ablates the heart clock, but also abolishes 24hr oscillations in cardiac mTOR activity and protein synthesis (26). Moreover, mTOR and protein synthesis are chronically activated in BMAL1 knockout hearts, associated with age-onset hypertrophic cardiomyopathy and reduced lifespan (20, 22, 26, 46). Such observations highlight the importance of normal circadian orchestration for maintenance of cardiac form and function.

The purpose of the present study was to determine whether the time-of-day at which dietary BCAA are consumed impacts a physiologic response (cardiac growth), as well as the potential pathologic implications of such a phenomenon. Here, we report that consumption of a BCAA-enriched meal specifically at the end of the active period causes a rapid growth of the heart, which is dependent on the cardiomyocyte circadian clock. Moreover, repetitive consumption of BCAA-enriched meals at the end of the active period (i.e., daily for a 6wk period) accelerated adverse remodeling and dysfunction in mice subjected to transverse aortic constriction. These observations provide support for the concept that BCAA-enriched meals should be avoided prior to sleep, particularly in at-risk individuals.

2. METHODS

2.1. Mice.

A total of 924 mice on the C57BL6/J background were utilized in the present study; 595 wild-type (Jackson Labs), 166 cardiomyocyte-specific Bmal1 knockout (CBK; $Bmal1^{flox/flox}$/MHCαCre$^{+/-}$), and 163 littermate control (CON; $Bmal1^{flox/flox}$/MHCαCre$^{-/-}$) mice. The CBK mouse model has been described previously (12). All experimental mice were male and were housed by the Animal Resources Program at the University of Alabama at Birmingham (UAB), under temperature-, humidity-, and light- controlled conditions. A strict 12-hour light/12-hour dark cycle regime was enforced (lights on at 6AM; zeitgeber time [ZT] 0); the light/dark cycle was maintained throughout these studies, facilitating investigation of diurnal variations (as opposed to circadian rhythms). Unless otherwise stated, mice were housed in standard microisolator cages, and provided standard rodent chow in an *ad libitum* fashion. All mice had free access to water. At the time of tissue and blood collection, age-matched mice (20wk) were anesthetized with pentobarbital. All animal experiments were approved by the Institutional Animal Care and Use Committee of the University of Alabama at Birmingham.

2.2. Dietary Composition.

Mice were allowed access to either a low BCAA diet (Teklad custom diet TD.150662) or a high BCAA diet (Teklad custom diet TD.170323); see Supplemental Table 1 for full nutritional details of these diets. Briefly, the high BCAA diet has leucine, isoleucine, and valine contents that are approximately 2-fold higher than a standard rodent chow. The low BCAA diet has leucine, isoleucine, and valine contents that are approximately 3-fold lower than a standard rodent chow. As such, BCAA contents are approximately 6-fold different between the low and high BCAA diets. A subset of studies also utilized a normal BCAA diet, with BCAA contents equivalent to a standard rodent chow (Teklad custom diet TD.140711). These three diets were formulated in a manner such that macronutrient content,

nitrogen content, and caloric density were essentially identical, by adjusting levels of distinct non-essential amino acids (alanine, asparagine, aspartate, glutamate, glutamine, glycine, proline, and serine). Importantly, none of the amino acid adjustments in these diets are considered below minimal nutritional requirements for mice.

2.3. Feeding Interventions.

Diets were provided to mice in either *ad libitum* or time-of-day-dependent manners. The time-of-day-dependent feeding protocol was performed either acutely or chronically. In the acute study (illustrated in Supplemental Fig. 1A), mice were initially fed the low BCAA diet for a 1 week period in an *ad libitum* fashion, after which they were divided into four experimental groups: 1) early high BCAA (EHB) meal fed; 2) early low BCAA (ELB) meal fed; 3) late high BCAA (LHB) meal fed; and 4) late low BCAA (LLB) meal fed. At ZT8, access to food was prevented for EHB and ELB mice; fasting was maintained for a 4hr period. At ZT12 (*i.e.*, the light-to-dark phase transition), mice in the EHB group were allowed access to the high BCAA diet for 4hrs. Conversely, mice in the ELB group were allowed access to the low BCAA diet during this time period. At ZT16 (*i.e.*, 4hrs into the dark phase), blood and hearts were collected from both EHB and ELB mice (i.e., immediately after the high and low BCAA meal, respectively). Next, food access was prevented for mice in the LHB and LLB groups at ZT16. At ZT20, mice in the LHB group were allowed access to the high BCAA diet for 4hrs. Conversely, mice in the LLB group were allowed access to the low BCAA diet during this time period. At ZT24 (*i.e.*, the dark-to-light transition), blood and hearts were collected from both LHB and LLB mice (i.e., immediately after the high and low BCAA meal, respectively). The purpose of the two 4hr fasting periods was to facilitate gastric emptying prior to, and encourage food consumption upon, subsequent food access. In a subset of acute studies, encapsulated rapamycin (42ppm; Rapamycin Holdings, Inc) was added to the low or high BCAA diets, to investigate the impact of inhibiting mTOR signaling; encapsulated vehicle (Eudragit) served as a control.

In the chronic study (illustrated in Supplemental Fig. 1B), mice were divided into one of two experimental groups: 1) early high BCAA (EHB) fed; and 2) late high BCAA (LHB) fed. All mice were allowed access to the low BCAA diet between ZT0 (*i.e.*, dark-to-light phase transition) and ZT8 (*i.e.*, 8hrs into the light phase). At ZT8, access to food was prevented for all mice; fasting was maintained for a 4hr period. At ZT12 (*i.e.*, the light-to-dark phase transition), mice in EHB group were allowed access to the high BCAA diet for 4hrs. Conversely, mice in the LHB groups were allowed access to the low BCAA diet during this time period. At ZT16 (*i.e.*, 4hrs into the dark phase), access to food was prevented for all mice; fasting was maintained for 4hrs. At ZT20, mice in the EHB group were allowed access to the low BCAA diet for 4hrs. Conversely, mice in the LHB group were allowed access to the high BCAA diet during this time period. Feeding regimes were maintained for either a 4wk (littermate flox-control and CBK mice) or 6wk (pressure overload study) period through use of a Comprehensive Laboratory Animal Monitoring System (CLAMS; Columbus Instruments Inc., Columbus, OH); each cage possesses two distinct feeders that open/close in a computer-controlled fashion. Upon completion of the study, blood and hearts were collected at one of two time points (ZT16 and ZT24).

2.4. Transverse Aortic Constriction (TAC).

Aortic banding was performed as described previously (42). Briefly, mice were anesthetized with 2% isoflurane, placed in the supine position, and fur was removed from above the sternum. A horizontal skin incision ~1 cm in length at the level of the suprasternal notch was made followed by an ~0.5 cm longitudinal cut in the proximal portion of the sternum. The muscle underneath the sternum was separated and the thymus was lifted out of the way to visualize the aortic arch. TAC was implemented by placement of a metal clip calibrated to a 30-gauge diameter needle between the innominate artery and the left common carotid artery. The muscle, sternum, and skin were sutured closed and povidone iodine was applied to the outer wound. The sham procedure was identical except that the aortic arch was not constricted. 24hrs post-surgery, success was determined by assessing pressure gradients via echocardiography. The feeding intervention was initiated 72hrs post-surgery and continued for a 6wk period.

2.5. Whole Body and Cardiac Parameters in vivo.

Food/caloric intake, energy expenditure, and physical activity were assessed continuously through use of a CLAMS. Lean and fat body masses were assessed by quantitative magnetic resonance (QMR, Echo 3-in-1, Echo Medical System) at an established UAB core facility. Glucose tolerance was assessed by administration of glucose (2g/Kg I.P.) in 6hr fasted mice, followed by measurement of blood glucose levels 0, 30, 60, 90, and 120 minutes post glucose injection using a Freestyle Lite glucometer (Abbott Laboratories, Abbott Park, IL). Insulin tolerance was assessed by administration of insulin (0.5U/Kg I.P.) in 6hr fasted mice, followed by measurement of blood glucose levels 0, 30, 60, 90, and 120 minutes post insulin injection using a Freestyle Lite glucometer. Cardiac function was assessed by echocardiography (at the UAB Echocardiography Core) using a VisualSonics VeVo 3100 Imaging System (VisualSonics, Toronto, Canada), and was analyzed by VisualSonics software.

2.6. Plasma BCAA Levels.

Plasma and cardiac BCAA levels were quantified by gas chromatography mass spectrometry (GCMS) analysis, as described previously (40).

2.7. Western Blotting.

Qualitative analysis of protein expression and phosphorylation status was performed via standard western blotting procedures, as described previously (11). Briefly, 10–30 μg protein lysate was separated on polyacrylamide gels and transferred to PVDF membranes. Membranes were probed for the following targets: p-mTOR$^{Ser-2448}$, p-P70S6K$^{Thr-389}$, p-S6$^{Ser-240/244}$, p-4EBP1$^{Thr-37/46}$, p-eIF4B$^{Ser-406}$, BCKDHa, p-BCKDHa$^{Ser-293}$, RAGA/B, RAGC, GβL, DEPTOR and RAGD (Cell Signaling; 2974, 9206, 2215, 9459, 8151, 90198, 40368, 4357, 5466, 3274, and 11816; Abcam 187679 respectively). Rabbit and mouse HRP-conjugated secondary antibodies (Cell Signaling, 7074 and 7076 respectively) were used for chemiluminescent detection with Luminata Forte Western Blotting substrate (Millipore, WBLUF0100). All densitometry data were normalized to calsequestrin (Abcam; ab3516). Importantly, due to the nature of time course studies, in order to minimize the contribution

that position on the gel might have on outcomes, samples were randomized on gels; samples were re-ordered post-imaging, only for the sake of illustration of representative images (note, all bands for representative images for an individual experiment were from the same gel; original images are presented in Supplemental Figure 7).

2.8. Protein Synthesis.

Protein synthesis was assessed by monitoring incorporation of puromycin into cardiac proteins, as described previously (32). Briefly, mice were injected with puromycin (40nmol/g body weight), followed by heart isolation 45min later; puromycin incorporation was determined through Western Blotting.

2.9. Histologic Assessment.

Cross sections from the medial heart were taken immediately upon removal of heart and fixed in formalin for 24hrs. Wheat germ agglutinin (WGA) staining was utilized for measurement of myocyte cross-sectional area; at least 45 myocytes were assessed per heart using Image-J software (NIH), as described previously (18). Picrosirius Red staining of collagen fibers was utilized for semi-quantitative measurement of left ventricular fibrosis, using ImagePro Plus software (Media Cybernetics, Inc., Rockville, MD), as described previously (12).

2.10. Quantitative RT-PCR.

RNA was extracted from hearts using standard procedures (9). Candidate gene expression analysis was performed by quantitative RT-PCR, using previously described methods (14, 17). For quantitative RT-PCR, specific Taqman assays were designed for each gene from mouse sequences available in GenBank or were purchased from Thermo Fisher Scientific USA. All RT-PCR data were normalized to a combined trio of housekeeping genes (*Ppia*, *Actb*, *Rplp0*), and are presented as fold change from an indicated reference group.

2.11. Statistical analysis.

Statistical analyses were performed using two-way ANOVA, as described previously (6, 7). Briefly, analyses were performed using Prism statistical software to investigate main effects of time, genotype and/or treatment, followed by a Sidak post hoc analyses for pair-wise comparisons (indicated in Figures). Cosinor analyses were performed to determine whether 24hr time series data significantly fit a cosine curve; if they did, then mesor (daily average value), amplitude (peak-to-mesor difference), and acrophase (timing of the peak) were calculated, as described previously (29). In all analyses, the null hypothesis of no model effects was rejected at $p<0.05$. For figures reporting 24hr variations in a parameter, it is noteworthy that ZT0 and ZT24 are identical, and that the data are double plotted (purely for the sake of presentation); statistical analyses were performed in the absence of a ZT24 time point.

3. RESULTS

3.1. Effects of Dietary BCAA Manipulation on Cardiac and Whole Body Parameters.

The overall goal of the present study was to determine whether the time-of-day at which dietary BCAAs are consumed impacts cardiac physiology/pathology. In an attempt to identify appropriate diets for subsequent time-of-day-dependent studies, we first characterized the effects of feeding mice diets with distinct BCAA contents (in an *ad libitum* manner) on whole body and cardiac parameters. Age-matched mice were initially fed a standard rodent chow. At 12-wk of age, hearts were isolated from a sub-set of mice (termed baseline group), whereas the remaining mice were fed one of three distinct diets with differing BCAA contents (in an *ad libitum* manner): 1) low BCAA diet (0.33x); 2) normal BCAA diet (1x); or 3) high BCAA diet (2x). Both body weight and biventricular weight to tibia length ratio (BVW/TL) were significantly higher in mice fed normal or high BCAA diets for a 4wk period (relative to mice fed the low BCAA diet; Fig. 1A). In contrast, BW and BVW/TL ratio were comparable between mice fed a standard rodent chow (i.e., baseline), the normal BCAA diet, and the high BCAA diet (Fig. 1A). These data suggest that standard/normal rodent diets provide sufficient BCAAs to maintain body and cardiac masses, such that increasing dietary BCAAs above standard/normal levels (i.e., the high BCAA diet) has little impact (over a 4wk period) on these parameters in healthy mice.

We next performed a more thorough phenotypic characterization of the impact that low and high BCAA diets have on mice (ad libitum feeding for a 4wk period); these 2 diets were chosen for further interrogation due to largest differential outcomes on cardiac mass observed in Fig. 1Aii. Total daily caloric intake, macronutrient (protein, carbohydrate, fat) intake, physical activity, and energy expenditure did not differ between low versus high BCAA diet fed mice (Table 1). Consistent with the nature of the intervention, total daily BCAA intake was 84% lower in low versus high BCAA diet fed mice; this was associated with 52%, 41%, and 58% lower levels of plasma leucine, isoleucine, and valine in low versus high BCAA diet fed mice (Table 1). Despite similar caloric intake in low and high BCAA diet fed mice, low BCAA diet fed mice exhibited decreased body weight at the end of the 4wk feeding period (8% lower compared to high BCAA diet fed mice; Table 1). This was associated with significantly decreased fat body mass in low (versus high) BCAA diet fed mice, in the absence of alterations in lean body mass (Table 1). No differences were observed in either glucose or insulin tolerance between low and high BCAA diet fed mice (Supplemental Fig. 2). Collectively, these data suggest that feeding mice a low BCAA diet for 4wks modestly decreased body mass and adiposity (relative to high BCAA fed mice), in the absence of major perturbations in whole body metabolic homeostasis.

We next investigated the effects of dietary BCAA manipulation on the heart at functional, gravimetric, histologic, and molecular levels. Echocardiographic analysis revealed that hearts from low BCAA diet fed mice exhibited a modest reduction in left ventricular posterior wall thickness, stroke volume, cardiac output, and ejection fraction (relative to hearts from high BCAA diet fed mice), in the absence of alterations in other echocardiographic parameters (Table 1). Gravimetric analysis of hearts revealed that the BVW/TL ratio was reduced by 11% in low BCAA diet fed mice (relative to high BCAA diet

fed mice; Fig. 1B). Similarly, cardiomyocyte size was decreased by 34% in low BCAA diet fed mice (relative to high BCAA diet fed mice; Fig. 1C). Gene expression of the hypertrophic marker *Nppa* was significantly lower in hearts of low BCAA diet fed mice, in the absence of alterations in *Myh7* expression (relative to high BCAA diet fed mice; Fig. 1D). Finally, the mTOR signaling axis (Supplemental Fig. 3) was investigated, given that BCAA-induced activation of this pathway has previously been linked with cardiac growth (34); of the components investigated, p-p70S6K$^{Thr-389}$ and p-S6$^{Ser-240/244}$ were significantly decreased (by 39% and 33%, respectively) in hearts of low BCAA diet fed mice (relative to high BCAA diet fed mice; Fig. 1E). Collectively, these data are consistent with modest cardiac atrophy following restriction of dietary BCAA content over a 4wk period.

3.2. Cardiac Growth Specifically at the End of the Active Period in Response to Dietary BCAAs.

To interrogate the hypothesis that responsiveness of the heart to dietary BCAA is time-of-day-dependent, mice were initially fed the low BCAA diet for 1wk, in an attempt to reduce BCAA-mediated signaling in the heart to baseline levels. During this 1wk period, mice were singly housed in cages with wire bottom flooring; this 1wk period of acclimatization with the low BCAA diet modestly decreased body weight in mice (7% lower relative to baseline; Fig. 2A). Following a short (4hr) period of fasting, mice were immediately fed a single high BCAA meal during either the first 4hrs of the dark phase (i.e., early high BCAA; EHB) or during the last 4hrs of the dark phase (i.e., late high BCAA; LHB); mice fed low BCAA meals during these time periods served as controls (i.e., ELB and LLB for mice in early and late low BCAA meal groups, respectively; see illustration in Supplemental Fig. 1A). Total caloric intake during the 4hr meal was equal between all experimental groups (Fig. 2Bi). Consistent with the intervention, mice fed high BCAA meals consumed 5.8-fold more BCAAs compared to mice fed low BCAA meals, irrespective of time-of-day (Fig. 2Bii). Similarly, plasma BCAA levels were significantly higher in mice fed high BCAA meals (relative to those fed low BCAA meals; Fig. 2C). Importantly, no significant differences were observed in plasma BCAA levels between EHB and LHB mice (Fig. 2C). The impact of the 4-hr BCAA meal on the heart was assessed at functional, gravimetric, histologic, and molecular levels. At the functional level, cardiac output was significantly decreased in LHB mice (relative to LLB mice), in the absence of alterations in other echocardiographic parameters (Table 2). At the gravimetric level, a significant increase (12%) in BVW/TL was observed in LHB, but not in EHB, mouse hearts (relative to their respective controls; Fig. 2D). This occurred in the absence of body weight differences between LHB and EHB mice (Table 2). Histological analysis revealed that the high BCAA meal significantly increased cardiomyocyte size (73%) in LHB mice (compared to LLB controls), but not in EHB mice (Fig. 2E). Gene expression of *Nppa* and *Myh7* were not differ significantly between the experimental groups (Table 2). Collectively, these data reveal a rapid (within 4hrs) and dramatic (73%) increase in cardiomyocyte size when mice consume dietary BCAAs only at the end of the active (dark) period.

The rapid increase in cardiac mass and cardiomyocyte size at the end of the active period in response to dietary BCAAs could be secondary to numerous mechanisms. Consistent with a

lack of contribution of edema, no significant differences were observed in the wet weight to dry weight ratio for hearts in the different experimental groups (Supplemental Fig. 4). Given that BCAAs are known to promote protein synthesis, we next investigated whether BCAAs selectively augment cardiac protein synthesis at the end of the active period. Fig. 3A reveals that the high BCAA meal significantly increased cardiac protein synthesis (45%) in LHB mice (compared to LLB controls), but not in EHB mice. The protein synthesis inhibitor rapamycin was next utilized to establish whether increased cardiac growth in response to dietary BCAAs at the end of the active period was dependent on protein synthesis. Consistent with earlier studies (Fig. 2D–E), the BCAA meal at the end of the active period increased both BVW/TL ratio and cardiomyocyte size in vehicle treated mice; this effect was abolished in rapamycin treated mice (Fig. 3B–C). These observations are consistent with the hypothesis that BCAAs promote protein synthesis in the heart at the end of the active period, leading to cardiac growth.

BCAAs promote protein synthesis in part through activation of the mTOR signaling axis (Supplemental Fig. 3) (10, 44). Moreover, rapamycin is an established mTOR inhibitor (4). We therefore next assessed whether BCAA-induced mTOR signaling was selectively augmented in the heart at the end of the active period. As anticipated, a 2-way ANOVA revealed multiple significant main effects of the BCAA meal (i.e., diet main effect); phosphorylation status of all five mTOR signaling components investigated were increased by the BCAA meal (Fig. 3D). Time-of-day main effects were also observed for p-mTOR$^{Ser-2448}$ and p-S6$^{Ser-240/244}$; both these mTOR signaling axis components were augmented at the end of the active period (i.e., ZT24; Fig. 3D). Importantly, a post hoc analysis revealed significantly higher p-S6$^{Ser-240/244}$ in hearts of LHB mice (compared to hearts of EHB mice; Fig. 3Diii). In addition to BCAAs, the mTOR signaling axis can be activated by numerous growth factors, including insulin and insulin-like growth factor 1 (IGF1). Although plasma insulin levels were not significantly different between experimental groups, cardiac *Igf1* mRNA levels were significantly higher (73%) in LHB hearts (relative to EHB hearts; Fig 3E). Interestingly, a 2-way ANOVA revealed that cardiac ribosomal RNAs *18s* and *28s* are significantly increased (21% and 17%, respectively) at ZT24 compared to ZT16 (i.e., main effect of time-of-day; Fig. 3F). Collectively, data presented in Figures 2 and 3 are consistent with the hypothesis that the heart is primed for growth at the end of the active period, such that consumption of dietary BCAAs at this time results in cardiac hypertrophy.

3.3. Dynamics of Cardiac Growth in Response to Daily BCAA Meals.

Although our observations thus far suggest that dietary BCAAs selectively augment protein synthesis and growth of the heart at the end of the active period, several uncertainties remain. These include whether the growth response is: 1) dependent on an initial 1wk period of “BCAA deficiency”; 2) transient in nature; and/or 3) additive if dietary BCAAs are persistently consumed at the end of the active period for multiple successive days. To simultaneously address all of these questions, mice were fed a 4hr high BCAA meal either at the beginning (early high BCAA; EHB) or at the end (late high BCAA; LHB) of the dark phase on a daily basis for a 4wk period (as illustrated in Supplemental Fig. 1B); after 4wk, hearts were isolated at the end of the two 4hr meals (i.e., ZT16 and ZT24). Importantly, no

significant differences in body weight, total daily caloric intake, or total daily BCAA intake were observed between EHB and LHB fed mice (Fig. 4A–B). Total daily amount of BCAA intake was reduced by only approximately one third (relative to that observed for mice fed a normal BCAA content diet in an *ad libitum* fashion; Fig 4Bii). Consistent with the intervention, 80% of daily BCAA intake was between ZT12 and ZT16 in EHB mice, whereas 78% of daily BCAA intake was between ZT20 and ZT24 in LHB mice (Fig. 4Biii). Similarly, plasma leucine, isoleucine, and valine levels were higher at ZT16 in EHB mice, and were higher at ZT24 in LHB mice (Fig. 4C). Gravimetric and histologic analysis revealed increased BVW/TL ratio (16%) and cardiomyocyte size (75%) in LHB hearts (compared to EHB hearts) only at ZT24; at ZT16, no significant differences were observed between the two feeding groups (Fig. 4D–E). Western blot analysis identified significantly higher levels of p-mTOR$^{Ser-2448}$ (51%), p-p70S6K$^{Thr-389}$ (262%) and p-S6$^{Ser-240/244}$ (84%) in LHB hearts (compared to EHB hearts) only at ZT24 (Fig. 4F). In contrast, no significant diet-dependent effects were observed for p-4EBP1$^{Thr-37/46}$ or p-eIF4B$^{Ser-406}$ (Fig. 4F). Collectively, these data confirm that the heart is more sensitive to BCAA-induced growth at the end of the dark phase, and suggest that the hypertrophic response is highly dynamic (being reversed within 16 hours after cessation of the BCAA-enriched meal).

3.4. Increased Responsiveness of the Heart to Dietary BCAAs at the End of the Dark Phase is Governed by the Cardiomyocyte Circadian Clock.

To test the hypothesis that the cardiomyocyte circadian clock temporally modulates responsiveness of the heart to BCAA-induced mTOR activation and cardiac growth, cardiomyocyte-specific BMAL1 knockout (CBK) mice were employed. Initially, circadian clock component (*Arntl*, *Nr1d1*) and output (*Dbp*) genes were assessed in CBK and littermate control hearts collected at 4hr intervals across the 24hr day. Consistent with disruption of the circadian clock, 24-hr oscillations observed for these genes in control (CON) hearts were attenuated in CBK hearts (i.e., a 59%−63% reduction in amplitude; Fig. 5A and Supplemental Table 2). CBK mice were fed the high BCAA diet either at the beginning (EHB) or at the end (LHB) of the dark phase for a 4wk period (as described for CON mice in Section 3.3; see Supplemental Fig. 1B for an illustration of the protocol). Body weight, total daily caloric intake and total daily BCAA intake were similar between EHB and LHB fed CBK mice (Supplemental Fig. 5A–B). Consistent with the intervention (and observations made in CON mice; Fig. 4B), dietary BCAA intake was higher between ZT12 and ZT16 in CBK mice within the EHB group, whereas dietary BCAA intake was higher between ZT20 and ZT24 in CBK mice within the LHB group (Supplemental Fig. 5Biii). Similarly, plasma leucine, isoleucine, and valine levels were higher at ZT16 in the EHB group, and were higher at ZT24 in the LHB group (Supplemental Fig. 5C). Hearts were isolated at either ZT16 or ZT24, followed by assessment of cardiac mass, cardiomyocyte size, and mTOR signaling. BVW/TL ratio and cardiomyocyte size were not significantly different between EHB and LHB fed CBK mice, regardless of the time-of-day (Fig. 5B–C). Similarly, no significant differences in p-mTOR$^{Ser-2448}$, p-p70S6K$^{Thr-389}$, p-S6$^{Ser-240/244}$, p-4EBP1$^{Thr-37/46}$, or p-eIF4B$^{Ser-406}$ levels were observed between EHB versus LHB hearts, at either ZT16 or ZT24 (Fig. 5D). Collectively, these observations suggest that the cardiomyocyte circadian clock is required for time-of-day-dependent fluctuations in cardiac BCAA responsiveness.

3.5. Candidate Mechanistic Links between the Cardiomyocyte Circadian Clock and Cardiac BCAA Responsiveness.

Comparison of cardiac mass, cardiomyocyte size, and mTOR signaling in CBK (Fig. 5B–D) and CON (Fig. 4D–F) mice challenged with the EHB and LHB feeding regimes suggests that these parameters are chronically elevated in CBK hearts. We therefore directly compared cardiac mass and mTOR signaling in CBK and littermate CON hearts (isolated from mice fed a standard chow in an *ad libitum* manner). Despite identical body weights, BVW/TL ratio was significantly higher in CBK versus CON mice (Fig. 6A). Investigating mTOR signaling components at distinct times of the day revealed that p-mTOR$^{Ser-2448}$ exhibited an approximate 2-fold (trough-to-peak) oscillation in CON hearts, peaking at ZT22 (as determined by cosinor analysis); this oscillation was abolished in CBK hearts (Fig. 6Bii and Supplemental Table 2). Cosinor analysis revealed that p-eIF4B$^{Ser-406}$ also exhibited a significant oscillation in CON hearts, which peaked at ZT4 (Fig. 6Bv and Supplemental Table 2); this oscillation was abolished in CBK hearts (Fig. 6Bv and Supplemental Table 2). Surprisingly, daily fluctuations in p-P70S6k$^{Thr-389}$ were augmented in CBK hearts, with higher levels observed during the dark phase (Fig. 6Biii and Supplemental Table 2). No significant oscillations were observed for p-S6$^{Ser-240/244}$ or p-4EBP1$^{Thr-37/46}$ in either CBK or littermate control hearts (Fig. 6B and Supplemental Table 2). Importantly, a 2-way ANOVA revealed that p-mTOR$^{Ser-2448}$, p-S6$^{Ser-240/244}$, p-p70S6K$^{Thr-389}$, and p-eIF4B$^{Ser-406}$ were all significantly increased in CBK hearts relative to littermate controls (genotype main effect; Fig. 6B). These observations led us to hypothesize that CBK hearts may chronically exhibit increased sensitivity to dietary BCAAs (independent of time-of-day). To test this hypothesis, CBK and littermate control mice were fed either a low, normal, or high BCAA diet in an *ad libitum* fashion; after a 4wk period, hearts were isolated for gravimetric analysis. BVW/TL was 14.2% higher in CBK mice fed a normal BCAA diet (relative to littermate controls; Fig. 6C). In contrast, this genotype difference was attenuated in low BCAA fed mice (10.4% difference between CBK and littermate controls), and was exacerbated in high BCAA fed mice (16.1% difference between CBK and littermate controls; Fig. 6C). Collectively, these observations suggest that genetic disruption of the cardiomyocyte circadian clock may increase responsiveness of the heart to dietary BCAAs in a chronic manner (i.e., independent of the time of day).

We next set out to identify candidate mechanistic links between the cardiomyocyte circadian clock and cardiac BCAA responsiveness. Candidate mechanisms investigated include circadian clock regulation of: 1) cardiac BCAA catabolism; 2) cardiac amino acid and ribosomal RNA abundance; and 3) sensitivity of mTOR activation by amino acids. Prior studies suggest that the circadian clock transcriptionally regulates genes encoding for BCAA catabolism enzymes/modulators, potentially via KLF15 (47). Consistent with prior studies, *Klf15* mRNA exhibits a significant 24hr oscillation in control hearts, which is abolished in CBK hearts (Fig. 7Ai and Supplemental Table 2). Of the BCAA catabolism genes investigated, only *Ivd* exhibited a significant time-of-day-dependent oscillation in control hearts (which is abolished in CBK hearts; Fig. 7A and Supplemental Table 2). *Ivd*, *Bckdha*, *Klf15*, and *Bckdhb* mRNA levels were all significantly decreased in CBK (versus control) hearts (i.e., genotype main effect; Fig. 7A and Supplemental Fig. 6). Consistent with lower *Bckdha* mRNA levels, both BCKDH protein and p-BCKDHa$^{Ser-293}$ levels were

significantly decreased in CBK hearts (i.e., genotype main effect; Fig. 7A). Moreover, cardiac BCAA (and total amino acid) levels are significantly increased in CBK hearts (relative to CON hearts; genotype main effect), particularly at the end of the active period (ZT0; post hoc analysis) (Fig. 7B). Interestingly, cardiac total amino acid levels exhibit a significant 24hr oscillation in the heart, being 8% higher at ZT0 versus ZT12 (Fig. 7B and Supplemental Table 2). Similarly, *28s* rRNA significantly oscillates in CON hearts (cosinor analysis; Supplemental Table 2), being 20% higher at ZT0 versus ZT12, while *18s* rRNA is chronically increased in CBK hearts (genotype main effect; Fig. 7B). Next, we investigated multiple components of the ragulator-rag complex that are known to influence mTOR activation (particularly in response to amino acids); these included four RAG isoforms (RAG A/B/C/D) and GβL (21). Western blot and subsequent cosinor analysis revealed that none of these proteins exhibited significant 24hr oscillations in either CBK or control hearts (Fig. 7C, Supplemental Fig. 6, and Supplemental Table 2). However, a 2-way ANOVA revealed significantly elevated levels in RAGA, RAGD, and GβL in CBK hearts (i.e., genotype main effect; Fig. 7B). Recent reports suggest that DEPTOR attenuates responsiveness of mTOR to BCAAs in cardiomyocytes (15). Cosinor analysis revealed that DEPTOR protein levels peak at approximately ZT11 in control hearts, and that this 24hr rhythm is abolished in CBK hearts (Fig. 7Cv and Supplemental Table 2). Collectively, these observations are consistent with the hypothesis that temporal regulation of cardiac amino acid, ribosomal RNA and/or DEPTOR levels by the cardiomyocyte circadian clock may mediate daily rhythms in cardiac BCAA responsiveness, while genetic disruption of the cardiomyocyte circadian clock increases cardiac BCAA sensitivity through a combination of BCAA catabolism repression, increase in free amino acids and ribosomes, as well as induction of multiple ragulator-rag complex components.

3.6. Augmentation of Adverse Cardiac Remodeling by Consumption of BCAAs at the End of the Dark Phase in a Murine Model of Heart Disease.

Although repetitive consumption of a BCAA-enriched meal at the end of the active period did not have accumulative effects on cardiac growth in healthy mice, we tested the hypothesis that this feeding behavior may accelerate adverse remodeling and dysfunction during heart disease. Accordingly, our long-term EHB and LHB feeding protocol (Supplemental Fig. 1B) was performed in a murine model of pressure overload (i.e., transverse aortic constriction; TAC). One day after surgery, twelve TAC mice (with essentially identical pressure gradients) and twelve sham controls were assigned into EHB and LHB feeding groups (i.e., six mice in each of the four experimental groups). After 6wk, cardiac remodeling was assessed at functional, gravimetric, histologic, and molecular levels in surviving mice (two mice in the EHB TAC group died within 2 weeks post-surgery). Importantly, all assessments were performed at ZT4, to avoid acute effects of the BCAA meals (which ended at ZT16 in EHB mice and ZT24 in LHB mice). As predicted, a 2-way ANOVA revealed that TAC decreased both ejection fraction and fractional shortening, and increased left ventricular volume and inner diameter (during both diastole and systole; Fig. 8A). Importantly, these TAC-induced alterations in functional parameters were exacerbated in LHB mice, relative to EHB mice (Fig. 8A). Gravimetric analysis revealed that TAC significantly increased BVW/TL ratio in LHB, but not EHB, mice (Fig. 8B). Although the TAC-induced increase in cardiomyocyte size was similar between EHB and LHB mice at

ZT4 (Fig. 8C), the TAC-induced increase in fibrosis was significant only in LHB (but not EHB) mice (Fig. 8D). Molecular markers of cardiac hypertrophy (*Nppa* and *Myh7* mRNA) and fibrosis (*Col1a1* mRNA) were also induced to a greater extent in LHB mice following TAC (relative to EHB mice; Fig. 8E). Collectively, these data reveal that consumption of BCAA at the end of the active period worsens adverse remodeling and dysfunction during heart disease.

4. DISCUSSION

Caloric intake in excess of energy expenditure is associated with numerous cardiometabolic and cardiovascular diseases (5). In addition to total caloric intake, macro- (and micro-) nutrient content and sources (e.g., minimally processed fruits and vegetables versus differentially processed foods) are thought to be important variables for disease risk (23). For example, excess red meat consumption is associated with increased atherosclerosis risk, plausibly in part through trimethylamine-N-oxide generation via microbial carnitine metabolism (27). Red meat also serves as an enriched source of BCAA; elevated circulating BCAA levels are also considered significant risk factors for obesity, diabetes mellitus, and heart failure (25, 28, 37, 43). Recently, attention has turned towards understanding how the timing of nutrient intake impacts health. Interest in this concept arose in part following appreciation that metabolic pathways vary as a function of time-of-day, leading to suggestions that the metabolic fate of nutrients (e.g., oxidation versus storage) depends on intake timing. Early studies in rodent models reported that consumption of calorically dense, high fat diets towards the end of the awake period resulted in greater weight gain, adiposity, dyslipidemia, hyperinsulinemia, and cardiac dysfunction (compared to consumption of the same high fat meal at the beginning of the awake period) (2, 8, 39). Similarly, observational studies in humans suggest that the timing (and frequency) of meals impacts numerous cardiometabolic and CVD risk factors (35). Therefore, both the composition and timing of meals should be considered for optimal health.

Temporal partitioning of cardiac metabolism across the day has been studied extensively. Three main phases have been described: 1) increased oxidative metabolism at the beginning of the awake period (likely important for increased ATP synthesis during this period of increased contractility); 2) increased nutrient storage towards the end of the awake period (predicted to replenish glycogen and triglyceride stores in anticipation of the upcoming sleep phase fast); and 3) increased cellular constituent turnover (protein, phospholipids, etc) at the wake-to-sleep transition (which could be considered as a daily preventative maintenance, to promote normal organ function) (45). Although beneficial for cardiac function in most physiologic conditions, evidence is emerging that circadian governance may have pathologic consequences (31). For example, challenging mice with isoproterenol at the awake-to-sleep transition (a time of increased cellular constituent turnover) leads to greater adverse cardiac remodeling; the same isoproterenol challenge at the sleep-to-awake transition is without effect (12). Such observations suggest that the heart is primed for growth and remodeling at the end of the awake period, such that an inappropriate stimulus/stress at this time may be detrimental. We have recently reported that mTOR signaling is increased in the heart at the end of the active period, associated with increased cardiac protein synthesis rates at this time (26). Although the cardiomyocyte circadian clock appears to be critical for these time-of-

day-dependent rhythms, the mechanistic links between this molecular timekeeper and mTOR signaling remains unclear. BCAAs are established mTOR activators (44). Moreover, recent transcriptomic approaches suggest that multiple ragulator-rag complex components are circadian regulated, several of which transduce the BCAA signal to mTOR activation (e.g., *rragd*, encoding for RAGD) (46). Such observations led us to hypothesize that the cardiomyocyte circadian clock may modulate mTOR responsiveness to BCAA, thus ensuring cardiac growth and repair occur at a distinct time of the day.

Here, we confirm that the heart is primed for growth at the end of the active period, as evidenced by augmented *Igf1* mRNA (Fig. 3E), ribosomal RNAs (Fig. 3F and 7B), amino acids (Fig. 7B), and mTOR signaling (Fig. 6B) at this time of the day. Moreover, CBK hearts exhibit aberrant 24hr patterns in amino acid levels, ribosomal RNA and mTOR signaling, which are chronically elevated (Fig. 6B and 7B). This is consistent with increased protein synthesis and hypertrophic phenotype reported in CBK hearts (46). By feeding mice BCAA-enriched meals at specific times during the day, we revealed increased responsiveness of mTOR signaling to BCAA-induced activation at the end of the active period (versus beginning of the active period; Fig. 3D and 4F). These time-of-day-dependent differences in BCAA-induced mTOR signaling activation were lost in CBK hearts (Fig. 5D). Such observations are consistent with the concept that the cardiomyocyte circadian clock temporally governs BCAA responsiveness of the heart. In an attempt to identify potential molecular links between the cardiomyocyte circadian clock and BCAA responsiveness, multiple BCAA catabolism and ragulator-rag complex components were investigated, as well as cardiac amino acids and ribosomal RNA (Fig. 7). Of these, cardiac amino acid, ribosomal RNA, and DEPTOR levels exhibited significant 24hr oscillations (i.e., data fit a cosine curve; Supplemental Table 2), which is dependent on the cardiomyocyte circadian clock (Fig. 7B–C). Given that DEPTOR is an established repressor of mTOR activation, we postulate that low levels of DEPTOR at the end of the active period may promote growth and repair of the myocardium at this time. Interestingly, independent of the time-of-day, BCAA catabolism genes are chronically repressed in CBK hearts, concomitant with elevated cardiac BCAAs levels, consistent with prior reports of decreased leucine oxidation rates (16). We speculate that chronic BCAA catabolism repression, concomitant with increased amino acid, ribosomal RNA, and ragulator-rag complex components, will promote chronic activation of mTOR signaling and hypertrophic growth of CBK hearts.

The current study highlights several noteworthy concepts. The first relates to the timing of dietary BCAA intake during normal and disease states. Here, we report that feeding healthy mice a high BCAA meal at the end of the active period resulted in a striking 73% increase in cardiomyocyte size within 4hr. Such an observation highlights the dynamic nature by which cardiomyocytes can remodel in response to a single meal, and is akin to observations in the python heart (which similarly experiences a dramatic meal-induced hypertrophic response) (1). Importantly, we also report that this feeding strategy exacerbates adverse cardiac remodeling and contractile dysfunction in an established heart disease model (Fig. 8). Regarding translation potential of these observations, it is possible that healthy individuals may experience benefits from consuming BCAA-enriched meals at the end of the day (e.g., physiologic hypertrophic growth, as reported for skeletal muscle previously (38)), whereas at-risk individuals may accelerate cardiac disease development. Many diets have been

popularized, including intermittent fasting and ketogenic diets; the latter is often protein enriched, which will include BCAA. The current study highlights the need to consider the time-of-day at which a fasting period is terminated by consumption of a BCAA-enriched meal (dependent on the health status of the individual). Another translational consideration relates to chronopharmacology; by reinforcing the concept that cardiac growth occurs primarily at the end of the active period, the current study highlights the need to consider the most effective administration time for medications that reduce left ventricular hypertrophy (e.g., angiotensin-converting enzyme inhibitors) (30). Another potentially important observation is the apparent increased responsiveness of the heart to BCAA-induced ventricular growth following genetic disruption of the cardiomyocyte circadian clock. Given that shift workers exhibit increased cardiovascular disease risk (41), and that shift work disrupts circadian clocks (33), the possibility exists that shift workers are more susceptible to the adverse effects of excess dietary BCAA.

In summary, the current study reveals a striking increase in the sensitivity of the heart to BCAA-induced activation of the mTOR signaling and cardiomyocyte growth towards the end of the active period, which is dependent on the cardiomyocyte circadian clock. The observation that consumption of a BCAA-enriched meal at the end of the active period can rapidly (within hours) enlarge cardiomyocyte size, reveals the dynamic nature of the heart in response to a dietary intervention. Moreover, consumption of BCAA-enriched meals at the end of the active period augments cardiac disease development. Collectively, these studies are consistent with the concept that shifting food intake towards the beginning of the day is beneficial for reducing cardiac disease risk.

Supplementary Material

Refer to Web version on PubMed Central for supplementary material.

ACKNOWLEDGEMENTS

We would like to thank Maximiliano Grenett, Anna Larussa, and Stephanie Reed for technical assistance, and David B. Allison for constructive comments. Graphic abstract was created with BioRender.com.

5. COMPETING INTERESTS STATEMENT

This work was supported by the National Heart, Lung, and Blood Institute (R01HL123574 and R01HL122975 for MEY; T32HL129948 for SDP; F32HL154531 for MNL).

8. REFERENCES

1. Andersen JB, Rourke BC, Caiozzo VJ, Bennett AF, and Hicks JW. Physiology: postprandial cardiac hypertrophy in pythons. Nature 434: 37–38, 2005. [PubMed: 15744290]
2. Arble DM, Bass J, Laposky AD, Vitaterna MH, and Turek FW. Circadian timing of food intake contributes to weight gain. Obesity (Silver Spring) 17: 2100–2102, 2009. [PubMed: 19730426]
3. Asher G and Sassone-Corsi P. Time for Food: The Intimate Interplay between Nutrition, Metabolism, and the Circadian Clock. Cell 161: 84–92, 2015. [PubMed: 25815987]
4. Ballou LM and Lin RZ. Rapamycin and mTOR kinase inhibitors. J Chem Biol 1: 27–36, 2008. [PubMed: 19568796]
5. Bhupathiraju SN and Hu FB. Epidemiology of Obesity and Diabetes and Their Cardiovascular Complications. Circ Res 118: 1723–1735, 2016. [PubMed: 27230638]

6. Bray M, Shaw C, Moore M, Garcia R, Zanquetta M, Durgan D, Jeong W, Tsai J, Bugger H, Zhang D, Rohrwasser A, Rennison J, Dyck J, Litwin S, Hardin P, Chow C, Chandler M, Abel E, and Young M. Disruption of the circadian clock within the cardiomyocyte influences myocardial contractile function; metabolism; and gene expression. Am J Physiol Heart Circ Physiol 294: H1036–H1047, 2008. [PubMed: 18156197]
7. Bray MS, Ratcliffe WF, Grenett MH, Brewer RA, Gamble KL, and Young ME. Quantitative analysis of light-phase restricted feeding reveals metabolic dyssynchrony in mice. Int J Obes (Lond) 37: 843–852, 2013. [PubMed: 22907695]
8. Bray MS, Tsai JY, Villegas-Montoya C, Boland BB, Blasier Z, Egbejimi O, Kueht M, and Young ME. Time-of-day-dependent dietary fat consumption influences multiple cardiometabolic syndrome parameters in mice. Int J Obes (Lond) 34: 1589–1598, 2010. [PubMed: 20351731]
9. Chomczynski P and Sacchi N. Single-step method of RNA isolation by acid guanidinium thiocyanate-phenol-chloroform extraction. Anal Biochem 162: 156–159, 1987. [PubMed: 2440339]
10. Cummings NE and Lamming DW. Regulation of metabolic health and aging by nutrient-sensitive signaling pathways. Molecular and cellular endocrinology 455: 13–22, 2017. [PubMed: 27884780]
11. Durgan DJ, Pat BM, Laczy B, Bradley JA, Tsai JY, Grenett MH, Ratcliffe WF, Brewer RA, Nagendran J, Villegas-Montoya C, Zou C, Zou L, Johnson RL Jr., Dyck JR, Bray MS, Gamble KL, Chatham JC, and Young ME. O-GlcNAcylation, novel posttranslational modification linking myocardial metabolism and cardiomyocyte circadian clock. J Biol Chem 286: 44606–44619, 2011. [PubMed: 22069332]
12. Durgan DJ, Tsai JY, Grenett MH, Pat BM, Ratcliffe WF, Villegas-Montoya C, Garvey ME, Nagendran J, Dyck JR, Bray MS, Gamble KL, Gimble JM, and Young ME. Evidence suggesting that the cardiomyocyte circadian clock modulates responsiveness of the heart to hypertrophic stimuli in mice. Chronobiol Int 28: 187–203, 2011. [PubMed: 21452915]
13. Fontana L, Cummings NE, Arriola Apelo SI, Neuman JC, Kasza I, Schmidt BA, Cava E, Spelta F, Tosti V, Syed FA, Baar EL, Veronese N, Cottrell SE, Fenske RJ, Bertozzi B, Brar HK, Pietka T, Bullock AD, Figenshau RS, Andriole GL, Merrins MJ, Alexander CM, Kimple ME, and Lamming DW. Decreased Consumption of Branched-Chain Amino Acids Improves Metabolic Health. Cell reports 16: 520–530, 2016. [PubMed: 27346343]
14. Gibson UE, Heid CA, and Williams PM. A novel method for real time quantitative RT-PCR. Genome Res 6: 995–1001, 1996. [PubMed: 8908519]
15. González-Terán B, López JA, Rodríguez E, Leiva L, Martínez-Martínez S, Bernal JA, Jiménez-Borreguero LJ, Redondo JM, Vazquez J, and Sabio G. p38γ and δ promote heart hypertrophy by targeting the mTOR-inhibitory protein DEPTOR for degradation. Nature communications 7: 10477–10477, 2016.
16. He L, Hamm JA, Reddy A, Sams D, Peliciari-Garcia RA, McGinnis GR, Bailey SM, Chow CW, Rowe GC, Chatham JC, and Young ME. Biotinylation: a novel posttranslational modification linking cell autonomous circadian clocks with metabolism. Am J Physiol Heart Circ Physiol 310: H1520–1532, 2016. [PubMed: 27084392]
17. Heid CA, Stevens J, Livak KJ, and Williams PM. Real time quantitative PCR. Genome Res 6: 986–994, 1996. [PubMed: 8908518]
18. Ingle KA, Kain V, Goel M, Prabhu SD, Young ME, and Halade GV. Cardiomyocyte-specific Bmal1 deletion in mice triggers diastolic dysfunction, extracellular matrix response, and impaired resolution of inflammation. Am J Physiol Heart Circ Physiol 309: H1827–1836, 2015. [PubMed: 26432841]
19. Keith SW, Redden DT, Katzmarzyk PT, Boggiano MM, Hanlon EC, Benca RM, Ruden D, Pietrobelli A, Barger JL, Fontaine KR, Wang C, Aronne LJ, Wright SM, Baskin M, Dhurandhar NV, Lijoi MC, Grilo CM, DeLuca M, Westfall AO, and Allison DB. Putative contributors to the secular increase in obesity: exploring the roads less traveled. Int J Obes (Lond) 30: 1585–1594, 2006. [PubMed: 16801930]
20. Khapre RV, Kondratova AA, Patel S, Dubrovsky Y, Wrobel M, Antoch MP, and Kondratov RV. BMAL1-dependent regulation of the mTOR signaling pathway delays aging. Aging 6: 48–57, 2014. [PubMed: 24481314]
21. Laplante M and Sabatini DM. Regulation of mTORC1 and its impact on gene expression at a glance. J Cell Sci 126: 1713–1719, 2013. [PubMed: 23641065]

22. Lefta M, Campbell KS, Feng HZ, Jin JP, and Esser KA. Development of dilated cardiomyopathy in Bmal1-deficient mice. Am J Physiol Heart Circ Physiol 303: H475–485, 2012. [PubMed: 22707558]

23. Lichtenstein AH, Appel LJ, Brands M, Carnethon M, Daniels S, Franch HA, Franklin B, Kris-Etherton P, Harris WS, Howard B, Karanja N, Lefevre M, Rudel L, Sacks F, Van Horn L, Winston M, and Wylie-Rosett J. Diet and lifestyle recommendations revision 2006: a scientific statement from the American Heart Association Nutrition Committee. Circulation 114: 82–96, 2006. [PubMed: 16785338]

24. Lynch CJ and Adams SH. Branched-chain amino acids in metabolic signalling and insulin resistance. Nature reviews Endocrinology 10: 723–736, 2014.

25. Magnusson M, Lewis GD, Ericson U, Orho-Melander M, Hedblad B, Engström G, Ostling G, Clish C, Wang TJ, Gerszten RE, and Melander O. A diabetes-predictive amino acid score and future cardiovascular disease. European heart journal 34: 1982–1989, 2013. [PubMed: 23242195]

26. McGinnis GR, Tang Y, Brewer RA, Brahma MK, Stanley HL, Shanmugam G, Rajasekaran NS, Rowe GC, Frank SJ, Wende AR, Abel ED, Taegtmeyer H, Litovsky S, Darley-Usmar V, Zhang J, Chatham JC, and Young ME. Genetic disruption of the cardiomyocyte circadian clock differentially influences insulin-mediated processes in the heart. J Mol Cell Cardiol 110: 80–95, 2017. [PubMed: 28736261]

27. Naghipour S, Cox AJ, Peart JN, Du Toit EF, and Headrick JP. Trimethylamine-N-Oxide: Heart of the microbiota-cardiovascular disease nexus? Nutr Res Rev: 1–64, 2020.

28. Newgard CB, An J, Bain JR, Muehlbauer MJ, Stevens RD, Lien LF, Haqq AM, Shah SH, Arlotto M, Slentz CA, Rochon J, Gallup D, Ilkayeva O, Wenner BR, Yancy WS Jr., Eisenson H, Musante G, Surwit RS, Millington DS, Butler MD, and Svetkey LP. A branched-chain amino acid-related metabolic signature that differentiates obese and lean humans and contributes to insulin resistance. Cell metabolism 9: 311–326, 2009. [PubMed: 19356713]

29. Peliciari-Garcia RA, Bargi-Souza P, Young ME, and Nunes MT. Repercussions of hypo and hyperthyroidism on the heart circadian clock. Chronobiol Int 35: 147–159, 2018. [PubMed: 29111822]

30. Portaluppi F, Tiseo R, Smolensky MH, Hermida RC, Ayala DE, and Fabbian F. Circadian rhythms and cardiovascular health. Sleep Med Rev 16: 151–166, 2012. [PubMed: 21641838]

31. Rana S, Prabhu SD, and Young ME. Chronobiological Influence Over Cardiovascular Function: The Good, the Bad, and the Ugly. Circ Res 126: 258–279, 2020. [PubMed: 31944922]

32. Ravi V, Jain A, Ahamed F, Fathma N, Desingu PA, and Sundaresan NR. Systematic evaluation of the adaptability of the non-radioactive SUnSET assay to measure cardiac protein synthesis. Scientific reports 8: 4587, 2018. [PubMed: 29545554]

33. Resuehr D, Wu G, Johnson RL Jr., Young ME, Hogenesch JB, and Gamble KL. Shift Work Disrupts Circadian Regulation of the Transcriptome in Hospital Nurses. J Biol Rhythms 34: 167–177, 2019. [PubMed: 30712475]

34. Sciarretta S, Forte M, Frati G, and Sadoshima J. New Insights Into the Role of mTOR Signaling in the Cardiovascular System. Circ Res 122: 489–505, 2018. [PubMed: 29420210]

35. St-Onge MP, Ard J, Baskin ML, Chiuve SE, Johnson HM, Kris-Etherton P, Varady K, American Heart Association Obesity Committee of the Council on L, Cardiometabolic H, Council on Cardiovascular Disease in the Y, Council on Clinical C, and Stroke C. Meal Timing and Frequency: Implications for Cardiovascular Disease Prevention: A Scientific Statement From the American Heart Association. Circulation 135: e96–e121, 2017. [PubMed: 28137935]

36. Sun H and Wang Y. Branched chain amino acid metabolic reprogramming in heart failure. Biochim Biophys Acta 1862: 2270–2275, 2016. [PubMed: 27639835]

37. Tobias DK, Lawler PR, Harada PH, Demler OV, Ridker PM, Manson JE, Cheng S, and Mora S. Circulating Branched-Chain Amino Acids and Incident Cardiovascular Disease in a Prospective Cohort of US Women. Circ Genom Precis Med 11: e002157–e002157, 2018. [PubMed: 29572205]

38. Trommelen J and van Loon LJ. Pre-Sleep Protein Ingestion to Improve the Skeletal Muscle Adaptive Response to Exercise Training. Nutrients 8, 2016.

39. Tsai JY, Villegas-Montoya C, Boland BB, Blasier Z, Egbejimi O, Gonzalez R, Kueht M, McElfresh TA, Brewer RA, Chandler MP, Bray MS, and Young ME. Influence of dark phase restricted high fat feeding on myocardial adaptation in mice. J Mol Cell Cardiol 55: 147–155, 2013. [PubMed: 23032157]
40. Vaillant F, Lauzier B, Ruiz M, Shi Y, Lachance D, Rivard ME, Bolduc V, Thorin E, Tardif JC, and Des Rosiers C. Ivabradine and metoprolol differentially affect cardiac glucose metabolism despite similar heart rate reduction in a mouse model of dyslipidemia. Am J Physiol Heart Circ Physiol 311: H991–h1003, 2016. [PubMed: 27496881]
41. Vyas MV, Garg AX, Iansavichus AV, Costella J, Donner A, Laugsand LE, Janszky I, Mrkobrada M, Parraga G, and Hackam DG. Shift work and vascular events: systematic review and meta-analysis. BMJ 345: e4800, 2012. [PubMed: 22835925]
42. Wende AR, Kim J, Holland WL, Wayment BE, O'Neill BT, Tuinei J, Brahma MK, Pepin ME, McCrory MA, Luptak I, Halade GV, Litwin SE, and Abel ED. Glucose transporter 4-deficient hearts develop maladaptive hypertrophy in response to physiological or pathological stresses. Am J Physiol Heart Circ Physiol 313: H1098–H1108, 2017. [PubMed: 28822962]
43. Yang R, Dong J, Zhao H, Li H, Guo H, Wang S, Zhang C, Wang S, Wang M, Yu S, and Chen W. Association of branched-chain amino acids with carotid intima-media thickness and coronary artery disease risk factors. PloS one 9: e99598–e99598, 2014. [PubMed: 24910999]
44. Yang Z and Ming XF. mTOR signalling: the molecular interface connecting metabolic stress, aging and cardiovascular diseases. Obes Rev 13 Suppl 2: 58–68, 2012. [PubMed: 23107260]
45. Young ME. Temporal partitioning of cardiac metabolism by the cardiomyocyte circadian clock. Experimental physiology 101: 1035–1039, 2016. [PubMed: 27474266]
46. Young ME, Brewer RA, Peliciari-Garcia RA, Collins HE, He L, Birky TL, Peden BW, Thompson EG, Ammons BJ, Bray MS, Chatham JC, Wende AR, Yang Q, Chow CW, Martino TA, and Gamble KL. Cardiomyocyte-specific BMAL1 plays critical roles in metabolism, signaling, and maintenance of contractile function of the heart. J Biol Rhythms 29: 257–276, 2014. [PubMed: 25238855]
47. Zhang L, Prosdocimo Domenick A, Bai X, Fu C, Zhang R, Campbell F, Liao X, Coller J, and Jain Mukesh K. KLF15 Establishes the Landscape of Diurnal Expression in the Heart. Cell reports 13: 2368–2375, 2015. [PubMed: 26686628]

HIGHLIGHTS

1. The heart is primed for growth at the end of the active period.
2. BCAAs stimulate rapid growth of the heart at the end of the active period.
3. Eating BCAAs at the end of the active period exacerbates cardiac disease.

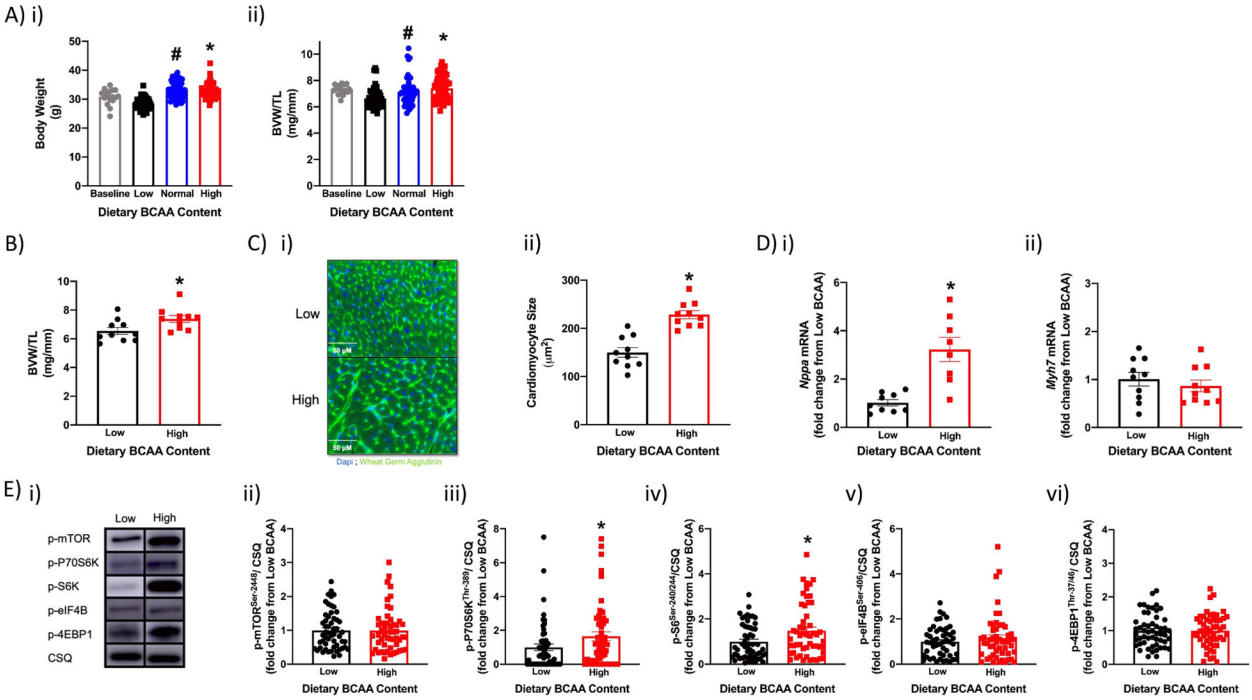

Figure 1. Whole body and cardiac parameters in wild-type mice fed diets with distinct BCAA contents for a 4wk period (in an *ad libitum* fashion).

(A) Body weight (i) and biventricular weight to tibia length (BVW/TL) ratio (ii) of mice at baseline (12wks old; n=18) and 4wks after *ad libitum* feeding with diets containing low, normal, or high BCAA levels (0.33x, 1x, or 2x relative to standard rodent chow, respectively; n=53–54). (B) BVW/TL ratio of mice fed low or high BCAA diets in an *ad libitum* manner for 4wks (n=10). (C) Cardiomyocyte size of mice fed low or high BCAA diets in an *ad libitum* manner for 4wks (n=10). (D) Cardiac *Nppa* (i) and *Myh7* (ii) mRNA levels of mice fed low or high BCAA diets in an *ad libitum* manner for 4wks (n=9–10). (E) Representative images (i) and quantification of p-mTOR$^{Ser-2448}$ (ii), p-p70S6K$^{Thr-389}$ (iii), p-S6$^{Ser-240/244}$ (iv), p-4EBP1$^{Thr-37/46}$ (v), and p-eIF4B$^{Ser-406}$ (vi) protein levels in hearts of mice fed low or high BCAA diets in an *ad libitum* manner for 4wks (n=53–54). Data/samples were collected at six distinct times of the day (with even distribution of sample sizes at the different ZTs; A, E), or only at ZT4 (B, C, D). All data are reported as mean ± SEM. *, $p<0.05$ for mice fed low versus high BCAA diets; #, $p<0.05$ for mice fed low versus normal BCAA diets.

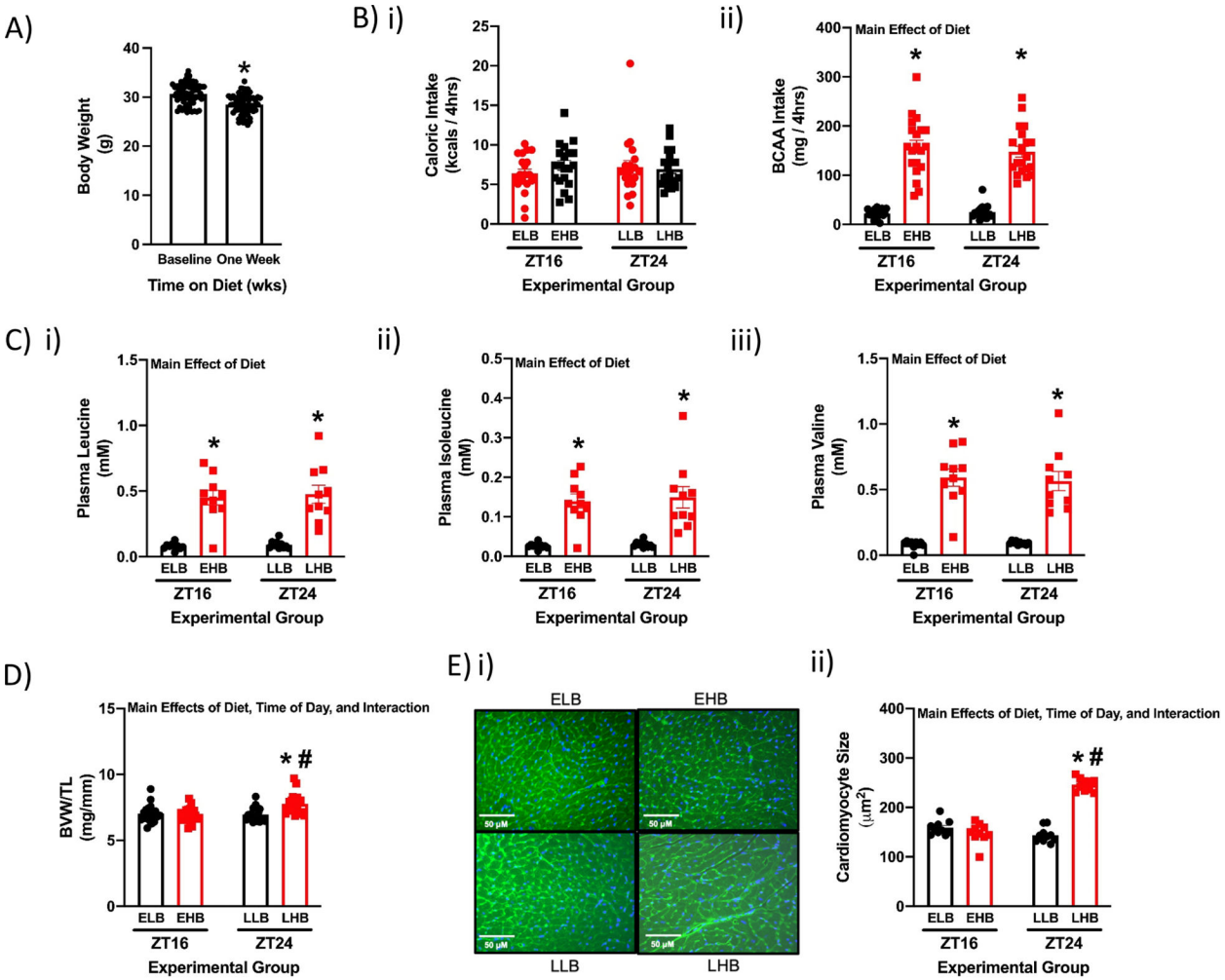

Figure 2. A single BCAA-enriched meal at the end of the active period increases cardiac growth in wild-type mice.

(A) Body weight in mice at baseline and 1 week after *ad libitum* feeding with the low BCAA diet (n=64). (B) Total caloric intake (i) and total BCAA intake (ii) during the 4hr meal in ELB (Early Low BCAA), EHB (Early High BCAA), LLB (Late Low BCAA), and LHB (Late High BCAA) fed mice (n=20). (C) Plasma leucine (i), isoleucine (ii), and valine (iii) levels at the end of the 4hr meal (n=10). (D) BVW/TL ratio at the end of the 4hr meal (n=20). (E) Cardiomyocyte size at the end of the 4hr meal (n=10). Data/samples were collected at ZT16 and ZT24. All data are reported as mean ± SEM. Main effects of diet, time-of-day, and/or interaction are reported at the top of the figure panels. *, $p<0.05$ for EHB versus ELB or LHB versus LLB (i.e., high BCAA meal effect within a ZT); #, $p<0.05$ for LHB versus EHB (i.e., high BCAA meal effect between ZTs); $, $p<0.05$ for 0 versus 1 week of low BCAA diet consumption (*ad libitum*).

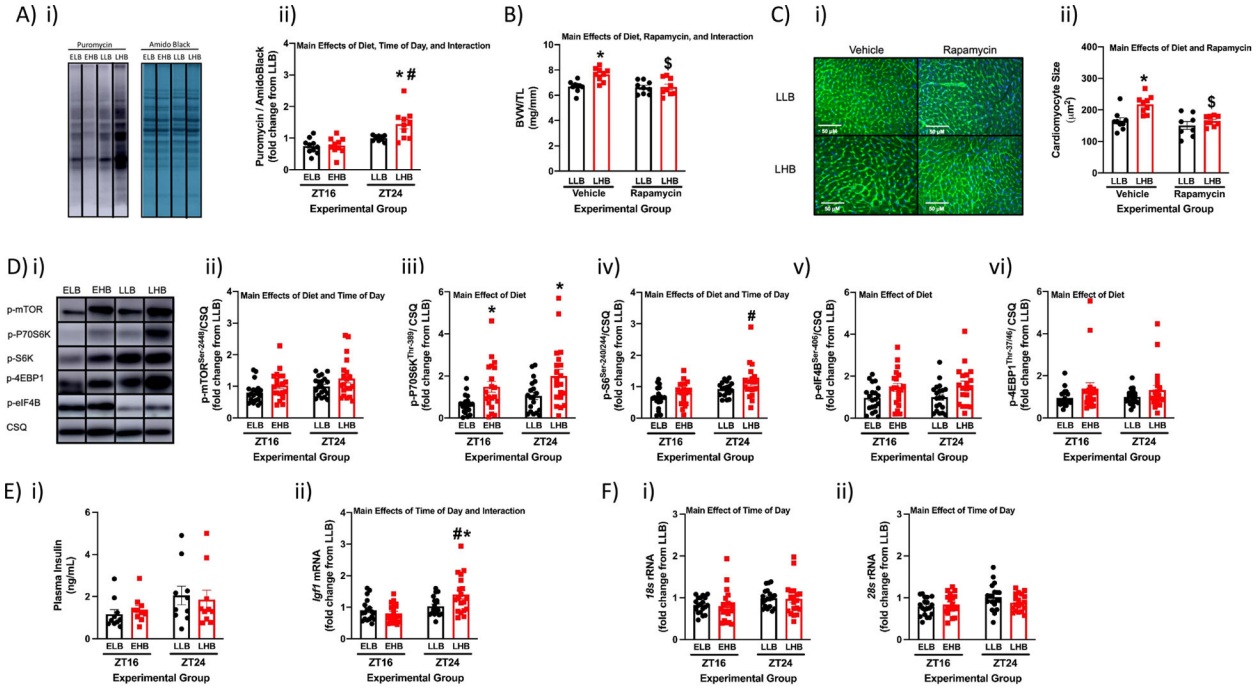

Figure 3. Role of mTOR signaling in BCAA-induced cardiac growth at the end of the active period in wild-type mice.

(A) Representative image (i) and quantification (ii) of puromycin incorporation into cardiac proteins during the 4hr meal in ELB (Early Low BCAA), EHB (Early High BCAA), LLB (Late Low BCAA), and LHB (Late High BCAA) fed mice (n=10). (B) BVW/TL ratio in LLB and LHB mice with or without rapamycin (42ppm) administration (n=9). (C) Cardiomyocyte size in LLB and LHB mice with or without rapamycin (42ppm) administration (n=8–9). (D) Representative images (i) and quantification of p-mTOR$^{Ser-2448}$ (ii), p-p70S6K$^{Thr-389}$ (iii), p-S6$^{Ser-240/244}$ (iv), p-4EBP1$^{Thr-37/46}$ (v), and p-eIF4B$^{Ser-406}$ (vi) protein levels in hearts of ELB, EHB, LLB, and LHB fed mice (n=20). (E) Plasma insulin (i; n=10) and cardiac *Igf1* mRNA (ii; n=18–19) levels in ELB, EHB, LLB, and LHB fed mice. (F) Cardiac *18s* (i) and *28s* (ii) rRNA levels in ELB, EHB, LLB, and LHB fed mice (n=19). Data/samples were collected at ZT16 and ZT24 (A, D, E, F), or only ZT24 (B, C). All data are reported as mean ± SEM. Main effects of diet, time-of-day, and/or interaction are reported at the top of the figure panels. *, $p<0.05$ for EHB versus ELB or LHB versus LLB (i.e., high BCAA meal effect within a ZT); #, $p<0.05$ for LHB versus EHB (i.e., high BCAA meal effect between ZTs); $, $p<0.05$ for LHB Vehicle versus LHB Rapamycin.

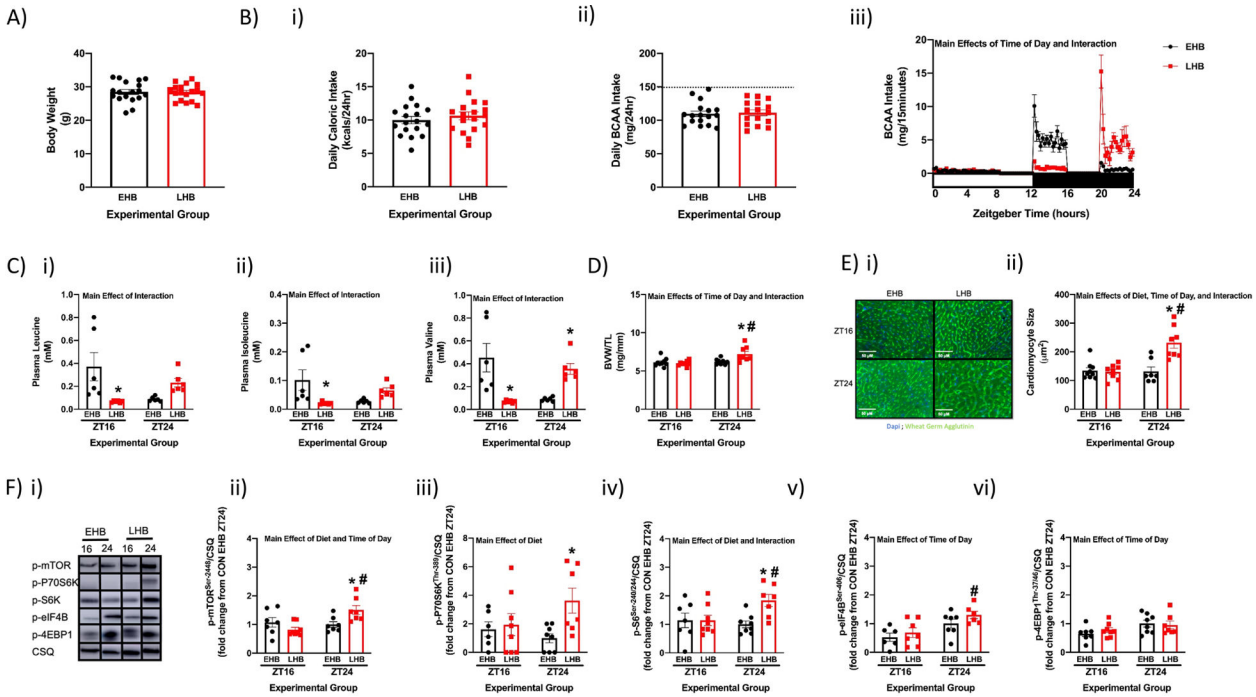

Figure 4. Feeding flox control (CON) mice daily BCAA enriched meals for a prolonged period (4 weeks) reveals persistent increased responsiveness of the heart to dietary BCAA at the end of the active period.

(A) Body weight after 4wks of feeding CON mice a daily 4hr BCAA meal during either the early (EHB) or late (LHB) portion of the active/dark phase (n=18). (B) Total daily caloric intake (i) and total daily BCAA intake (ii) during the 4wk feeding period, as well as time-of-day fluctuations in BCAA intake (iii); the horizontal dashed line in panel (ii) represents average total daily BCAA intake in mice fed a normal BCAA diet in an *ad libitum* manner (n=16–18). (C) Plasma leucine (i), isoleucine (ii), and valine (iii) levels for EHB and LHB fed CON mice (n=6). (D) BVW/TL ratio of hearts isolated from EHB and LHB fed CON mice (n=8–9). (E) Cardiomyocyte size of hearts isolated from EHB and LHB fed CON mice (n=7–9). (F) Representative images (i) and quantification of p-mTOR$^{Ser-2448}$ (ii), p-p70S6K$^{Thr-389}$ (iii), p-S6$^{Ser-240/244}$ (iv), p-4EBP1$^{Thr-37/46}$ (v), and p-eIF4B$^{Ser-406}$ (vi) protein levels in hearts isolated from EHB and LHB fed CON mice (n=6–8). Data/samples were collected at ZT4 (A, Bi, Bii), or at ZT16 and ZT24 (C, D, E, F), or at 15min intervals over the 24hr day (through use of a CLAMS; Biii). All data are reported as mean ± SEM. Main effects of diet, time-of-day, and/or interaction are reported at the top of the figure panels. *, $p<0.05$ for EHB versus LHB (i.e., high BCAA meal effect within a ZT); #, $p<0.05$ for ZT16 versus ZT24 (i.e., time-of-day effect within a BCAA meal feeding group).

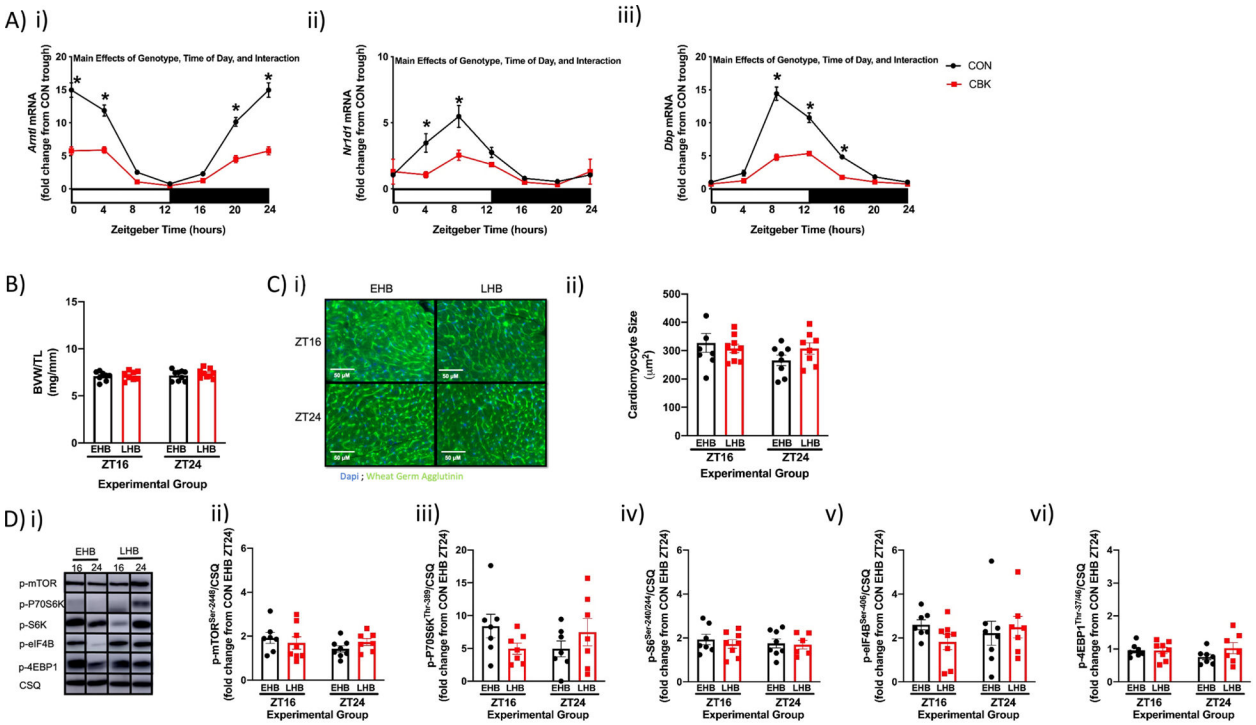

Figure 5. Feeding cardiomyocyte-specific BMAL1 knockout (CBK) mice daily BCAA enriched meals for a prolonged period (4 weeks) reveals dependence of increased responsiveness of the heart to dietary BCAA at the end of the active period on the cardiomyocyte circadian clock.

(A) Time-of-day fluctuations in mRNA levels of *Arntl* (i), *Nr1d1* (ii), *and Dbp* (iii) in hearts isolated from CBK and littermate flox control (CON) mice fed a standard rodent chow *ad libitum* (n=7–8). (B) BVW/TL ratio of hearts after 4wks of feeding CBK mice a daily 4hr BCAA meal during either the early (EHB) or late (LHB) portion of the active/dark phase (n=8–9). (C) Cardiomyocyte size of hearts isolated from EHB and LHB fed CBK mice (n=6–9). (D) Representative images (i) and quantification of p-mTOR$^{Ser-2448}$ (ii), p-p70S6K$^{Thr-389}$ (iii), p-S6$^{Ser-240/244}$ (iv), p-4EBP1$^{Thr-37/46}$ (v), and p-eIF4B$^{Ser-406}$ (vi) protein levels in hearts isolated from EHB and LHB fed CBK mice (n=6–8). Data/samples were collected at six distinct times of the day (ZT0, ZT4, ZT8, ZT12, ZT16, ZT20; A) or at ZT16 and ZT24 (B, C, D). For data presented in panel A, ZT0 and ZT24 are identical (the data are double plotted purely for the sake of presentation). For data presented in panel D, data are shown as fold change from littermate control (CON) hearts collected at ZT24 from mice in the EHB feeding group. All data are reported as mean ± SEM. Main effects of genotype, time-of-day, and/or interaction are reported at the top of the figure panels. *, $p<0.05$ for CON versus CBK hearts within a ZT.

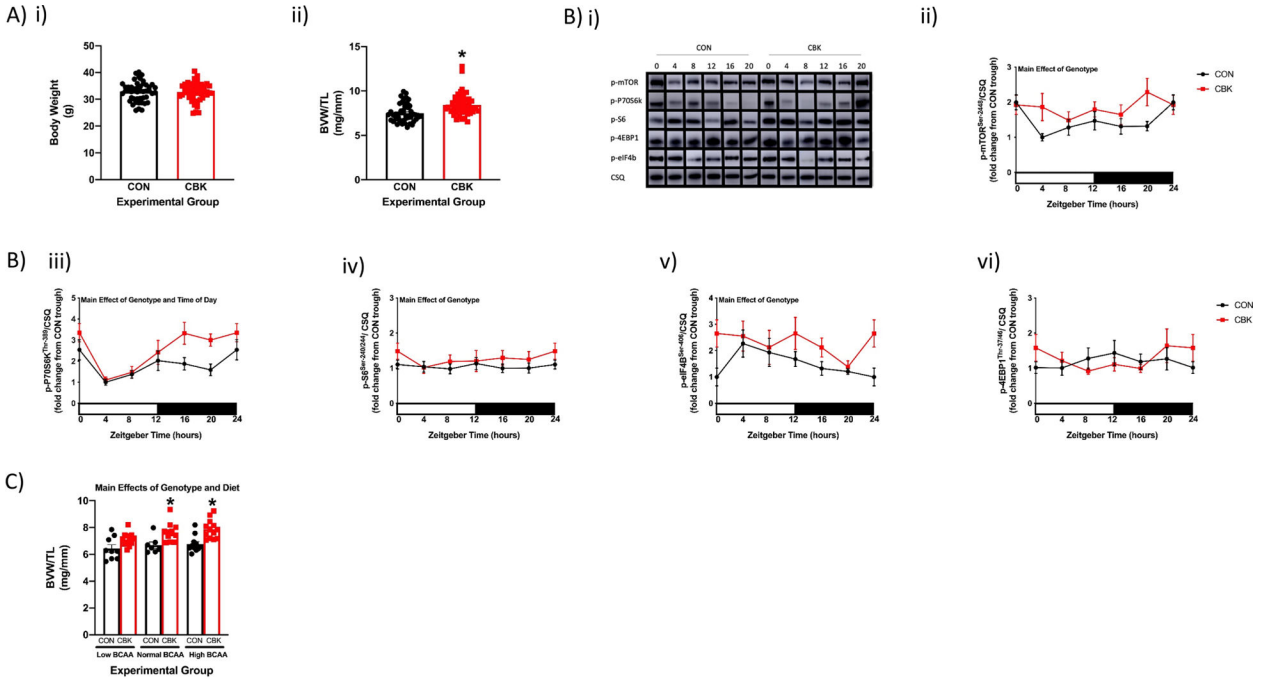

Figure 6. Chronic activation of the mTOR signaling axis in the heart of cardiomyocyte-specific BMAL1 knockout (CBK) mice, relative to littermate flox control (CON) mice.

(A) Body weight (i) and BVW/TL ratio (ii) in age-matched CBK and CON mice fed a standard rodent chow *ad libitum* (n=48–56). (B) Representative images (i) and quantification of p-mTOR$^{Ser-2448}$ (ii), p-p70S6K$^{Thr-389}$ (iii), p-S6$^{Ser-240/244}$ (iv), p-4EBP1$^{Thr-37/46}$ (v), and p-eIF4B$^{Ser-406}$ (vi) protein levels in hearts isolated from CBK and CON mice fed a standard rodent chow *ad libitum* (n=6–8). (C) BVW/TL ratio in CBK and CON mice 4wks after *ad libitum* feeding with diets containing low, normal, or high BCAA levels (0.33x, 1x, or 2x relative to standard rodent chow, respectively; n=7–13). Data/samples were collected at six distinct times of the day (ZT0, ZT4, ZT8, ZT12, ZT16, ZT20; A, B) or at ZT4 (C). For data presented in panel B, ZT0 and ZT24 are identical (the data are double plotted purely for the sake of presentation). Main effects of genotype, time-of-day, and/or diet are reported at the top of the figure panels. *, $p<0.05$ for CON versus CBK hearts.

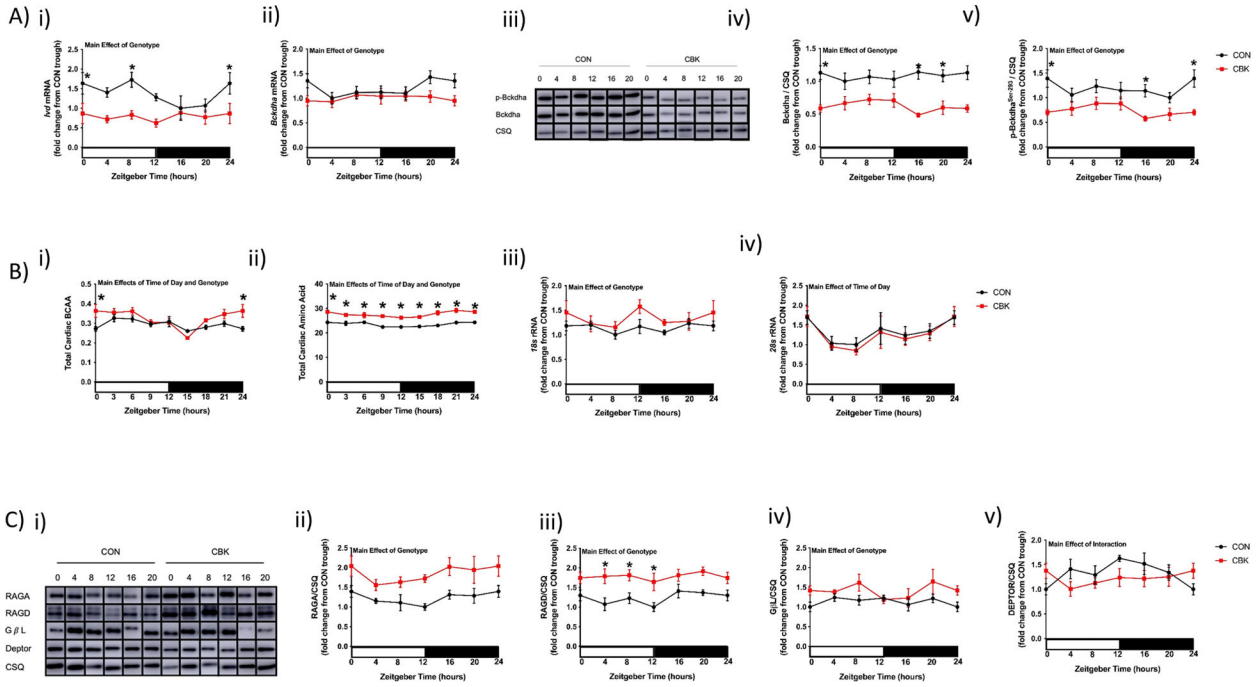

Figure 7. Alterations of BCAA catabolism components, amino acids, ribosomal RNAs, and regulator-rag complex components in the heart of cardiomyocyte-specific BMAL1 knockout (CBK) mice, relative to littermate flox control (CON) mice.

(A) Time-of-day fluctuations in *Ivd* mRNA (i), *Bckdha* mRNA (ii), BCKDHa protein (iv), and p-BCKDHa$^{Ser-293}$ protein (v) levels in hearts isolated from CBK and CON mice fed a standard rodent chow *ad libitum* (n=6–8); representative images for BCKDHa and p-BCKDHa$^{Ser-293}$ are shown in (iii). (B) Total BCAA (i), total amino acid (ii), *18s* rRNA (iii), and *28s* rRNA (iv) levels in hearts isolated from CBK and CON mice fed a standard rodent chow *ad libitum* (n=4–8). (C) Representative images (i) and quantification of RAGA (ii), RAGD (iii), GβL (iv), and DEPTOR (v) protein levels in hearts isolated from CBK and CON mice fed a standard rodent chow *ad libitum* (n=4–8). Data/samples were collected at either six distinct times of the day (ZT0, ZT4, ZT8, ZT12, ZT16, ZT20; A, Biii, Biv, C) or eight distinct times of the day (ZT0, ZT3, ZT6, ZT9, ZT12, ZT15, ZT18, ZT21; Bi, Bii); data for ZT0 and ZT24 are identical (the data are double plotted purely for the sake of presentation). Main effects of genotype, time-of-day, and/or interaction are reported at the top of the figure panels. *, $p<0.05$ for CON versus CBK hearts within a ZT.

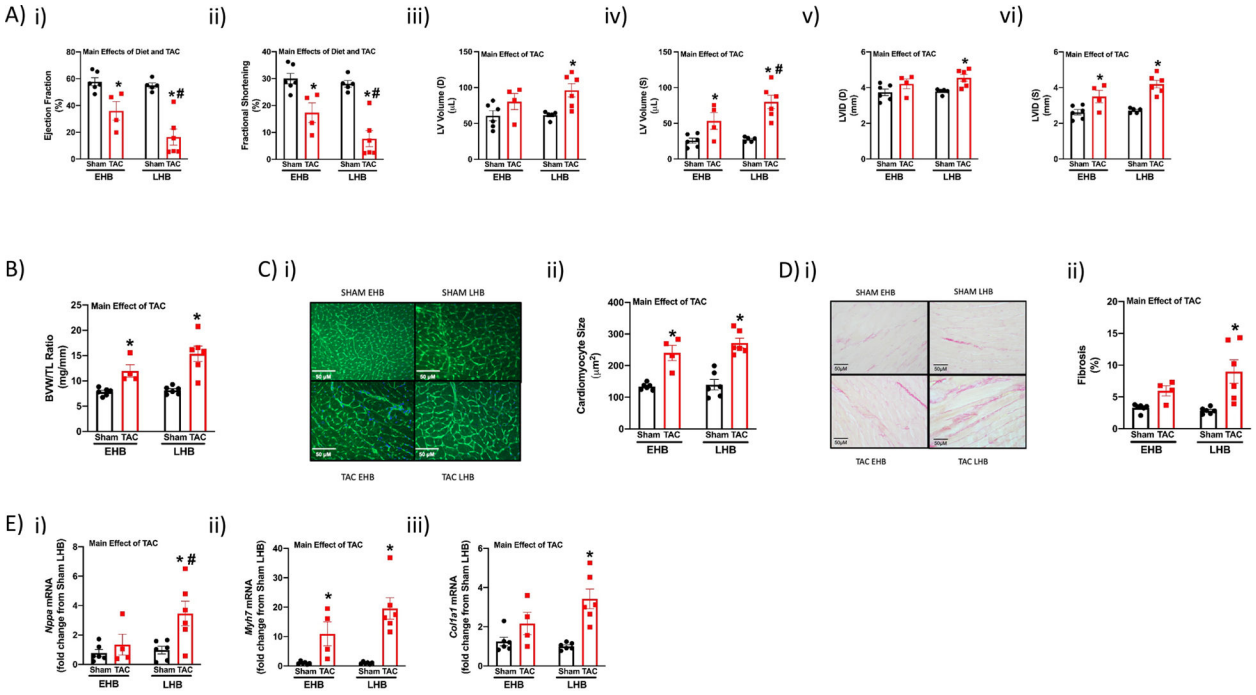

Figure 8. TAC-induced adverse cardiac remodeling is augmented by BCAA-enriched meals at the end of the active period in wild-type mice.

Mice underwent either TAC or sham surgery, followed by feeding of BCAA-enriched meals in a time-of-day-dependent manner (as illustrated in Supplemental Fig. 1B) for 6wk. (A) Echocardiographic assessment of cardiac function *in vivo* after 6wks of feeding TAC and sham mice a daily 4hr BCAA meal during either the early (EHB) or late (LHB) portion of the active/dark phase (n=4–6). (B) BVW/TL ratio of hearts isolated from EHB and LHB fed TAC/sham mice (n=4–6). (C) Cardiomyocyte size of hearts isolated from EHB and LHB fed TAC/sham mice (n=4–6). (D) Fibrosis of hearts isolated from EHB and LHB fed TAC/sham mice. (E) *Nppa* (i), *Myh7* (ii), and *Col1a1* (iii) mRNA levels in hearts isolated from EHB and LHB fed TAC/sham mice (n=4–6). All data/samples were collected at ZT4, and are reported as mean ± SEM. Main effects of TAC and diet are reported at the top of the figure panels. *, $p<0.05$ for TAC versus sham (within a feeding group); #, $p<0.05$ for LHB versus EHB (within a surgical group).

Table 1.

Whole body and cardiac parameters in wild-type mice fed diets with distinct BCAA contents for a 4wk period (in an *ad libitum* fashion).

Mice were fed either a low or high BCAA diet (0.33x or 2x relative to standard rodent chow, respectively) for a 4wk period. During the last week of feeding, whole body energy balance parameters were assessed through use of a CLAMS (continuous assessment throughout the 24hr day; n=7–8), body composition was assessed by QMR (at ZT4; n=7–8), cardiac function was assessed by echocardiography (at ZT4; n=9–10), and plasma was collected (at six distinct times of the day, with even distribution of sample sizes at the different ZTs; n=36) for measurement of plasma BCAAs by GCMS. All data are reported as mean ± SEM.

Parameter	Low BCAA	High BCAA
Total Daily Caloric Intake (kcal/24hr)	10.49±0.83	10.87±0.23
Total Daily Protein Intake (kcal/24hr)	2.29±0.18	2.43±0.06
Total Daily Carbohydrate Intake (kcal/24hr)	6.25±0.49	6.47±0.17
Total Daily Fat Intake (kcal/24hr)	1.94±0.15	2.06±0.05
Total Daily BCAA Intake (mg/24hr)	41.41±0.38	259.93±4.71*
Total Daily Energy Expenditure (kcal/24hr)	10.08±0.72	9.84±0.48
Total Daily Physical Activity (Beam Breaks; A.U.)	28,360±3,679	34,291±2,422
Body Weight (g)	28.65±0.50	31.20±1.00*
Fat Body Mass (g)	4.17±0.21	5.40±0.33*
Lean Body Mass (g)	22.79±0.50	23.77±0.54
Left Ventricular Posterior Wall Thickness (mm; S)	1.10±0.07	1.32±0.06*
Left Ventricular Posterior Wall Thickness (mm; D)	0.85±0.03	0.97±0.04
Intraventricular Septum (mm; D)	0.85±0.03	0.87±0.04
Intraventricular Septum (mm; S)	0.78±0.03	0.86±0.04
Left Ventricular Interior Diameter (mm; D)	3.89±0.11	3.94±0.07
Left Ventricular Interior Diameter (mm; S)	2.75±0.10	2.62±0.09
Fractional Shortening (%)	29.49±1.12	33.72±1.58*
Left Ventricular Volume (μl; D)	66.56±4.49	68.10±3.11
Left Ventricular Volume (μl; S)	28.94±2.47	25.59±2.28
Stroke Volume (ul)	27.06±1.84	34.63±1.52*
Cardiac Output (ml/min)	13.04±0.93	17.24±1.05*
Ejection Fraction (%)	45.47±2.31	54.47±1.65*
Plasma Leucine (mM)	69.58±3.55	143.78±13.20*
Plasma Isoleucine (mM)	31.47±1.93	53.49±3.24*
Plasma Valine (mM)	86.79±3.62	208.53±12.84

*, $p<0.05$ for mice fed low versus high BCAA diets.

Table 2.

A single BCAA-enriched meal at the end of the active period decreases cardiac output in wild-type mice.

Mice were singly housed in cages with wire bottom flooring for a 1wk acclimatization period, with access to the low BCAA diet *ad libitum*. Following a short (4hr) period of fasting, mice were immediately fed a single high BCAA meal during either the first 4hrs of the dark phase (i.e., early high BCAA; EHB) or during the last 4hrs of the dark phase (i.e., late high BCAA; LHB); mice fed low BCAA meals during these time periods served as controls (i.e., ELB and LLB for mice in early and late low BCAA meal groups, respectively; see illustration in Supplemental Fig. 1A). After the 4hr meal, body weight was determined gravimetrically (n=20), cardiac function was assessed by echocardiography (n=16), and hearts were collected for gene expression assessment by RT-PCR (represented as fold change from LLB; n=18–20). Data/samples were collected at ZT16 (ELB and EHB groups) and ZT24 (LLB and LHB groups). All data are reported as mean ± SEM.

Parameter	**ZT16**		**ZT24**	
	ELB	**EHB**	**LLB**	**LHB**
Body Weight (g)	28.61±0.63	29.34±0.49	28.98±0.52	30.01±0.39
Left Ventricular Posterior Wall Thickness (mm; S)	1.24±0.09	1.17±0.05	1.26±0.06	1.24±0.07
Left Ventricular Posterior Wall Thickness (mm; D)	0.98±0.08	0.93±0.06	0.90±0.05	0.92±0.07
Intraventricular Septum (mm; D)	1.00±0.07	1.03±0.05	0.99±0.05	1.11 ±0.04
Intraventricular Septum (mm; S)	1.30±0.07	1.40±0.07	1.40±0.06	1.41±0.03
Left Ventricular Interior Diameter (mm; D)	3.73±0.13	3.95±0.11	3.80±0.06	3.75±0.10
Left Ventricular Interior Diameter (mm; S)	2.77±0.15	2.94±0.08	2.66±0.07	2.75±0.11
Fractional Shortening (%)	26.02±2.11	25.41±1.08	29.96±1.49	26.98±1.31
Left Ventricular Volume (μl; D)	60.68±4.60	69.68±4.90	62.33±2.26	61.19±3.57
Left Ventricular Volume (μl; S)	30.66±3.38	34.15±2.02	26.42±1.53	29.41±2.63
Stroke Volume (ul)	30.02±2.57	35.53±3.48	35.90±1.91	31.78±1.63
Cardiac Output (ml/min)	16,047±1,512	18,266±1,465	19,641±881$^{\#}$	16,487±931*
Ejection Fraction (%)	51.09±3.36	50.47±1.71	29.96±1.49	53.06±2.10
Nppa mRNA (A.U.)	1.13±0.26	1.16±0.28	1.05±0.23	1.81±0.23
Myh7 mRNA (A.U.)	1.24±0.17	1.16±0.24	1.06±0.21	0.85±0.13

*, $p<0.05$ for EHB versus ELB or LHB versus LLB (i.e., high BCAA meal effect within a ZT);

$^{\#}$, $p<0.05$ for LHB versus EHB (i.e., high BCAA meal effect between ZTs).